ELSEVIER

Chemical Engineering Journal 73 (1999) 205–216

Chemical Engineering Journal

Modelling catalytic combustion of carbon monoxide and hydrocarbons over catalytically active wire meshes

Anders Fredrik Ahlström-Silversand[a,*], Claes Ulf Ingemar Odenbrand[b]

[a]*Katator AB, Ideon Research Park, Ole Römers väg 12, S-223 70 Lund, Sweden*

[b]*Department of Chemical Engineering II, Chemical Center, Lund University, Institute of Science and Technology, PO Box 124, S-221 00 Lund, Sweden*

Received 2 December 1996; received in revised form 30 July 1998; accepted 11 January 1999

Abstract

A new way of preparing catalytically active wire meshes through a thermal-spray technique is described. A metal substrate (e.g. Kanthal AF) was plasma-sprayed with a composite ceramic/polymer-powder. The polymer content of the sprayed layer was burnt off whereupon a well-defined macro-porosity was created. By treating the so obtained material with an alumina-sol the specific surface area could be increased by a factor of 50 or more. The ceramic layer was finally activated with precious metals through an impregnation step. A numerical model was developed to compare the performance of wire-mesh-, monolith- and pellets catalysts. The model describes the resistance to internal and external mass- and heat transfer and the effects of axial dispersion. The wire-mesh model was verified through experiments. Different evaluation parameters were derived to compare the catalyst performance relative to the catalyst volume, the geometric weight, the catalyst weight, the pressure drop and the temperature response. Wire-mesh catalysts offer the following advantages: high mass and heat transfer numbers, moderate pressure drop, insignificant effects of pore diffusion and axial dispersion, thermal and mechanical strength, geometric flexibility, excellent thermal response, simplicity in the catalyst recovery. The cost of a wire-mesh catalyst is expected to be competitive to other alternatives.

Keywords: Wire mesh; Catalytic combustion; Thermal spraying; Modelling; Monolith; Pellets

1. Introduction

It is commonly known that the mass- and heat transfer characteristics in a bed of catalyst pellets are superior to those in a monolith catalyst. The pressure drop of a pellets bed is however significantly higher than the pressure drop of a monolith catalyst. Monolith catalysts are therefore used in applications where an inherent sensitivity against a high pressure drop exists, e.g. in automotive applications and in catalytic devices for combustion and flue-gas cleaning [1–3].

Wire-mesh catalysts combine the excellent mass- and heat transfer characteristics of a pellets catalysts with a relatively low pressure drop, mainly attributed to the high porosity of the wire-mesh structure. Wire-mesh catalysts are commonly used in the production of nitric acid from ammonia (Pt/Rh-catalyst) and formaldehyde from methanol (Ag-catalyst) [4,5]. In these cases the wire mesh consists of homogeneous metal wires, which are woven together. Homogeneous wire meshes are extremely expensive and rather inactive, due to the low specific surface area (only a few m^2 per kg of catalyst).

It is possible to add catalytic activity to a wire mesh by a conventional wash-coating procedure [6]. The major drawback here is the poor mechanical strength of the ceramic layer. The ceramic layer may flake away under the influence of mechanical stresses and vibrations whereupon the catalyst is destroyed.

By depositing the ceramic material through a thermal spray-technique (e.g. flame spraying or plasma spraying) it is possible to obtain a ceramic layer with an excellent adhesion to the substrate. The bond strength (shear stress necessary for fracture) usually is between 15 and 60 N/mm^2. Thermal spraying has been utilised in catalyst preparation before, mainly for the production of Raney-nickel- and iron-catalysts for hydrocarbon processing e.g. [7–12]. The porosity and the specific surface area of an as-sprayed ceramic layer are normally extremely low. It is therefore not possible to obtain a satisfactory catalytic activity by

*Corresponding author. Tel.: +46-46-18-22-91; fax: +46-46-18-22-99; e-mail: fredriksilversand@katator.se

1385-8947/99/$ – see front matter
PII: S1385-8947(99)00029-7

simply impregnating the ceramic layer with a solution containing catalytically active materials, e.g. precious metals. Some researchers have therefore used the thermally sprayed ceramic layer as a substrate for a wash coat and a catalytically active material, e.g. on details in internal combustion engines [13].

Our research is focused on the possibilities of obtaining an as-sprayed ceramic layer with a high porosity and a high specific surface area. The specific surface area of the porous ceramic layer may be increased further in a second step by treating it with different sols or through an in situ precipitation method. Catalytic activity is added to the ceramic layer in a third step through an ordinary impregnation procedure.

The thin and shell-like design of the catalytically active layer enables an excellent utilisation of the active material, i.e. the effectiveness factor with respect to pore diffusion is rather high compared to a pellets catalysts. The combination of a relatively low catalyst weight and a high heat transfer number leads to a low thermal inertia of the wire-mesh catalysts, which is of great interest in certain applications, e.g. in start-up catalysts in automotive applications.

Porous wire-mesh catalysts can be used in a number of interesting applications, where they may replace or complement existing pellets- and monolith catalysts. Examples of interesting applications are:

- Purification of flue gases with respect to CO and hydrocarbons
- Two-way catalysts in automotive applications
- Three-way catalysts in automotive applications (especially start-up catalysts)
- Catalytic combustion in energy production
- Catalytic devices for de-odourisation (ammonia, amines etc.)
- Purification of ventilation air with respect to VOC
- Ammonia oxidation
- Selective catalytic reduction of nitrogen oxides (SCR)
- Partial oxidation reactions like the ones used in formaldehyde- and acetaldehyde production
- Steam reforming
- Water-gas reactions

The mass- and heat transfer characteristics of wire-mesh catalysts have been extensively studied by a number of researchers e.g. [14]. These studies have focused on homogeneous wire meshes, mainly Pt/Rh or Pt/Pd, for the production of nitric oxide (nitric acid production). In our case it is also necessary to take the effects of pore diffusion into consideration since our catalyst is porous and has a relatively high specific surface area. The effects of axial dispersion may decrease the conversion considerably, especially at low ratios between the flow rate and the cross-sectional area of the package of catalytically active wire meshes. The effects of axial dispersion must thus be implemented in the numerical model.

The aim of this study is to develop a numerical model to describe the combustion of CO and HC on porous catalytically active wire meshes under mass transfer controlled conditions and to verify the calculations with experimental data. The performance of different catalyst shapes (pellets, monolith-, and wire-mesh type catalyst) are also compared in the study.

2. Experimental

2.1. Catalyst preparation

The catalysts were prepared by plasma spraying the wire meshes with a mixture of alumina and polyamide, as described elsewhere [17]. The polyamide content was burnt off in a second step (800°C during 1 h) to create a well-defined macro-porosity of the ceramic layer. The specific surface area of the as-sprayed ceramic layer was too low (usually below 1 m^2/g) for most catalyst applications. The specific surface area can be increased by depositing ceramic material with a high specific area in the macro-porosity of the as-sprayed ceramic layer. This deposition process was performed through in situ precipitation or through sol treatment. In situ precipitation was performed by treating the porous ceramic layer with a saturated solution of $Al(NO_3)_3$ (aq). The ceramic layer was then subjected to ammonia vapour whereupon $Al(OH)_3$ was produced in the pore system. The alumina hydroxide was converted into pseudo-γ-Al_2O_3 with a high surface area through thermal treatment. By treating the porous ceramic layer with an alumina-sol containing alumina-particles of a size of 15 nm (Nyacol Colloidal alumina-sol) it was possible to increase the specific area significantly. By repeating the deposition process several times it was possible to increase the specific surface area of the ceramic layer by a factor of 50–100 [17]. The porous ceramic layer was finally activated through a conventional impregnation procedure with a solution containing precious metals. After impregnating the ceramic layer with the precious metals, the catalysts were dried (110°C, 2 h) and finally reduced in an atmosphere containing 10 vol% H_2 (balance N_2) at 800°C for 2 h. The composition of the catalyst layer is shown schematically in Fig. 1.

In this study we used wire meshes with a mesh number ranging from 8 to 20 Tylor-mesh. The corresponding thicknesses of the wires were between 0.5 and 0.9 mm. The wire meshes were coated with a ceramic/polymer layer (20 vol% of polyamide) with a thickness of 40–150 μm through plasma spraying. The polyamide content was burnt off and the porous ceramic layer was treated with alumina-sol twice. The specific surface area of the ceramic layer was around 25 m^2/g in each case. The porous layer was then impregnated with an aqueous solution containing a mixture of Pd (0.75 mol/l) and Pt (0.25 mol/l) and finally dried and reduced, as described above. The total metal loading was around 10 $\mu mol/m^2$.

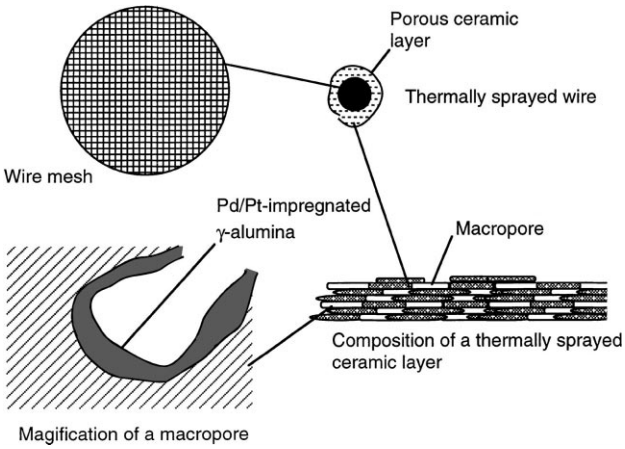

Fig. 1. Diagram showing the composition of the thermally sprayed wire-mesh structure.

2.2. Experimental procedure

The activity studies were carried out in a specially designed reactor, described in detail elsewhere [17]. The reactor consists of a tube with an inner diameter of 90 mm which is well insulated to avoid temperature gradients along the reactor. Air is supplied from a compressor system whereas nitrogen and carbon dioxide are supplied from gas cylinders. These gases are mixed in a system of valves and flow meters and the gas mixture is led into the reactor through a pre-heater. Water is supplied into a specially designed evaporation vessel in the reactor and the water vapour is mixed with the pre-heated gas mixture. Carbon monoxide and/or hydrocarbons are then added through a flow meter system and the resulting gas mixture is led through a couple of turbulence plates (to obtain a homogeneous gas mixture) and the catalyst holder. The catalyst holder contains a number of catalytically active wire meshes in series with an effective diameter of 85 mm. The temperature can be measured in the catalyst and at positions immediately before and after the catalyst. The catalyst temperature is the input signal to the temperature regulator.

Gas analysis is performed with a photo acoustic technique (Brüel Kjær Multigas analysator 201) and gas samples can be taken before and after the catalyst.

During the experiments the catalyst temperature was varied between 150°C and 600°C whereas the total flow ranged from 1 to 6 m^3/h (STP). The number of catalytically active wire meshes in series was varied between 1 and 5. In the experiments presented in this paper the gas mixture contained 2000 ppm of CO/hydrocarbons in air. The experiments were normally carried out in the totally mass transfer controlled region, indicated by the extremely weak temperature dependence of the observed reaction rate. A pseudo-first order behaviour with respect to the concentration was obtained for CO as well as for the hydrocarbons studied in the kinetically controlled region. Oxygen was present in a great excess whereby a zero-order behaviour was obtained.

2.3. Calculation of k_{ga} from experimental data

The mass transfer numbers were calculated directly from the conversion data obtained in the totally mass transfer controlled region ($x_{A,\,exp}$), the volume flow (V_0) and the total external surface area according to Eq. (1). The *j*-factor for mass transfer was calculated according to Eq. (2).

$$k_{ga} = \frac{V_0}{a_{ext} W} \ln\left(\frac{1}{1 - x_{A,\,exp}}\right), \tag{1}$$

$$J_D = \frac{\epsilon_w A_c}{a_{ext} W} \ln\left(\frac{1}{1 - x_{A,\,exp}}\right)\left(\frac{\nu}{D_g}\right)^{\frac{2}{3}}, \tag{2}$$

where $J_D = \frac{Sh}{Re\,Sc^{1/3}}$, $Re = \frac{dU}{\nu\epsilon_w}$.

2.4. Modelling wire-mesh catalysts

2.4.1. Reactor model

The calculations are based on a reactor model, which takes axial dispersion into consideration. Eq. (3) represent the dispersion model for a first-order reaction and the effects of axial dispersion is dependent on the axial dispersion coefficient (D_a), the superficial gas velocity (U) and the reactor length (L). The importance of axial dispersion increases as the reactor length and/or the gas velocity decreases. The conversion, x_A, can be determined by solving the second-order ordinary differential equation:

$$\frac{D_a}{UL}\frac{d^2x_A}{dz^2} - \frac{dx_A}{dz} + k\bar{t}(1 - x_A) = 0,\ z = \frac{l}{L},\ \bar{t} = \frac{L}{U}. \tag{3}$$

If the axial dispersion coefficient is close to zero the dispersion model approaches a plug-flow model. On the other hand, if D_a is a very large number, the dispersion model will approach a tank reactor model. Eq. (3) can be solved either numerically or analytically. The isothermal solution for a first-order reaction is given in Eq. (4)[18]. The calculations presented in this paper are based on this expression.

$$x_A = 1 - \frac{4a\,e^{((1/2)(UL/D_a))}}{(1 + a^2)\,e^{((a/2)(UL/D_a))} - (1 - a^2)\,e^{(-a/2)(UL/D_a)}},$$
$$a = \sqrt{1 + 4k\bar{t}(D_a/UL)}. \tag{4}$$

The axial dispersion coefficient, D_a, is dependent on the superficial gas velocity (U) and a characteristic diameter, i.e. the wire diameter. D_a can be derived from diagrams given by Levenspiel [18].

2.4.2. Kinetic expressions

The combustion reactions are modelled as first-order reactions with respect to CO and hydrocarbons and zero-order reactions with respect to oxygen. These assumptions are normally justified in flue-gas cleaning where the pollu-

tant gases are present only in low concentrations whereas oxygen is present in a great excess. The intrinsic reaction rate is defined according to Eq. (5) below. The pre-exponential factor, k_0, is assumed to be proportional to the specific surface area (S_a) of the catalyst and the coverage of active material (θ_{PM}).

$$r_{int} = k_0 \, e^{(-E_a/RT)} p_A^1 p_{O_2}^0, \; k_0 \propto S_a, \; \theta_{PM}. \tag{5}$$

The observed reaction rate is obtained by multiplying the intrinsic reaction rate with an over-all effectiveness factor (Ω) which compensates for boundary layer- and pore diffusion according to the following equation:

$$r_{obs} = \Omega r_{int}. \tag{6}$$

2.4.3. Mass- and heat transfer

The over-all effectiveness factor, Ω, is calculated from the effectiveness factor with respect to pore-diffusion (η), the surface dependent intrinsic reaction rate (k_v), the specific surface area (S_a), the mass transfer coefficient (k_{ga}) and the external surface area (a_{ext}) of the catalyst, according to Fogler [15].

$$\Omega = \frac{\eta}{1 + (\eta k_v S_a / k_{ga} a_{ext})}. \tag{7}$$

Satterfield and Cortex [14] have studied the mass transfer characteristics of homogeneous wire-mesh catalysts and have found a correlation between the *j*-factor for mass transfer and the Reynolds number according to Eq. (8a). Eq. (8b) should be used in cases of Reynolds numbers higher than 9 [15].

$$J_D = \frac{0.94}{Re^{0.717}}, \quad (0.4 < Re < 9), \tag{8a}$$

$$J_D = \frac{0.664}{Re^{0.57}\gamma^{0.43}}, \quad (3 < Re < 107), \; \gamma = (1 - Nd)^2. \tag{8b}$$

The porosity of the wire-mesh structure (ϵ_w) is calculated from a characteristic catalyst length (L), defined through Eq. (10), the mesh number (N) and the wire diameter (d). The wire-mesh porosity, ϵ_w, is normally above 0.7.

$$\epsilon_w = 1 - \frac{\pi L N^2 d}{4}, \tag{9}$$

$$L = \left(\frac{1}{N^2} + d^2\right)^{1/2}. \tag{10}$$

The external surface area of the catalyst can be calculated from the mesh number (N), the wire diameter (d), the number of wire meshes in series (n), the cross-section area (A_c) and the catalyst weight (W).

$$a_{ext} = \frac{n 2 N \pi d A_c}{W} = \frac{1}{t_c \rho_c}. \tag{11}$$

The effectiveness factor with respect to pore diffusion is evaluated from Thiele modulus (Φ) according to Eq. (12). Thiele modulus is calculated from the surface dependent intrinsic reaction rate (k_v), the specific surface area (S_a), the catalyst density (ρ_p), the effective diffusivity (D_{eff}) and the ratio between the catalyst volume and the exterior surface available for reactant penetration and diffusion (t).

$$\eta = \frac{3}{\Phi^2}(\Phi \cot h(\Phi) - 1), \tag{12}$$

$$\Phi = t\sqrt{\frac{k_v S_a \rho_p}{D_{eff}}}. \tag{13}$$

The effective diffusivity is obtained from the gas-phase diffusivity (D_g) the Knudsen diffusivity (D_k), the particle porosity (ϵ_p) and the tortousity factor (τ). The Knudsen diffusivity is in turn calculated according to Eq. (15).

$$D_{eff} = \left(\frac{1}{D_k} + \frac{1}{D_g}\right)^{-1} \frac{\epsilon_p}{\tau}, \tag{14}$$

$$D_k = 194 \frac{V_p}{S_a}\sqrt{\frac{T}{MW}}. \tag{15}$$

2.4.4. Pressure drop

The pressure drop of the wire-mesh catalyst is calculated with the Ergun equation, where the bed porosity is replaced with the wire-mesh porosity.

$$\Delta p = \rho U^2 \frac{nd}{\phi d} \frac{1 - \epsilon_w}{\epsilon_w^3}\left(\frac{150}{Re_w} + 1.75\right), \; Re_w = \frac{\phi \, d U}{\nu(1 - \epsilon_w)}. \tag{16}$$

2.4.5. Resistance to heat transfer

The heat transfer number (α) is estimated from the mass transfer number through the Chilton–Colburn analogy [22].

$$J_h = J_D, \; J_h = \frac{N}{Re \, Pr^{1/3}}, \; J_D = \frac{Sh}{Re \, Sc^{1/3}}. \tag{17}$$

From this analogy, the heat transfer number, can be obtained as:

$$\alpha = k_{ga} \frac{\lambda_a}{D_g}\left(\frac{Sc}{Pr}\right)^{1/3} \approx k_{ga} \frac{\lambda_a}{D_g}. \tag{18}$$

The ratio between Sc and Pr is close to unity whereupon the heat transfer number is obtained directly from the mass transfer number by multiplying it with the ratio between the thermal conductivity of air (λ_a) and the gas-phase diffusivity (D_g).

3. Results and discussion

3.1. Determination of a power-law expression for k_{ga} from experimental data

The mass transfer coefficient and the *j*-factor were calculated from the conversion data obtained in the totally mass

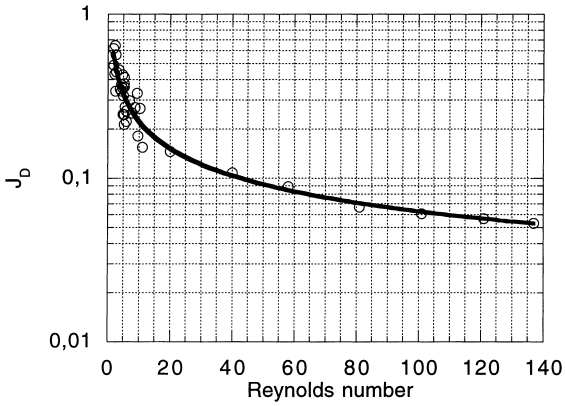

Fig. 2. The *j*-factor versus the Reynolds number, symbols representing experimental data and the line a power-law fit to the experimental data.

transfer controlled region according to Eqs. (1)–(3). As can be seen in Fig. 2, the experimental data are located in a corridor with a negative slope for increasing Reynolds numbers. By fitting a power-law expression to the total number of experimental data, the following expression was obtained:

$$J_D = \frac{0.78}{Re^{0.55}} \quad (0.8 < Re < 140). \tag{19}$$

The *j*-factor plot contains over 30 experimentally determined data where we have varied the mesh number, the number of wire meshes in series, the flow and the combustible compound. When comparing this expression with the ones proposed by Satterfied and Fogler it is obvious that the dependence of the Reynolds number is somewhat weaker in our case.

The *j*-factor is plotted versus the Reynolds number in Fig. 3. The corresponding values of the *j*-factor from Eqs. (8a) and (8b) are plotted in the same diagram. The values from Eq. (19) are in fair agreement with the expression proposed by Fogler at Reynolds numbers above 10. At Reynolds numbers below 10 the expression proposed by Satterfield gives a better agreement.

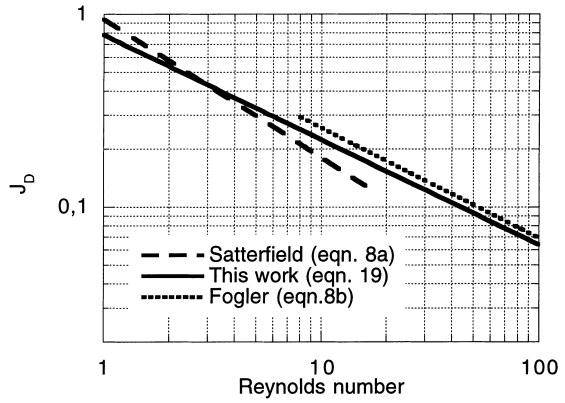

Fig. 3. Comparison of the experimentally derived *j*-factor-analogy with literature data.

According to our data it is thus possible to use the expressions proposed by Satterfied and Fogler to describe the mass transfer characteristics of catalytically active wire meshes prepared through a thermal-spray technique.

3.2. Kinetic data

The kinetic parameters in Eq. (5), i.e. E_a and k_0, were determined through regression analysis of experimental data obtained in the kinetically controlled region. The activation energy for CO-combustion was rather high, 290 kJ/mol whereas the activation energy for propylene- and terpene combustion were lower, 210 and 170 kJ/mol, respectively.

3.3. Verification studies

3.3.1. Combustion of different compounds

Combustion experiments were performed with different combustible compounds, i.e. carbon monoxide, propylene and terpenes (mainly α-pinen). During the experiments five catalytically active wire meshes (12 mesh) were placed in the catalyst holder and a gas containing 2000 ppm of combustible compound in air was led through the catalyst package at total flow rate of 2.4 m^3/h (STP). The gas was analysed with respect to hydrocarbons, carbon oxides and water and the conversion was calculated.

The wire meshes were coated with a porous alumina layer according to the earlier description with an average thickness of about 50 μm. The open porosity of the ceramic layer was approximately 40 vol% (measured through water penetration experiments). The specific surface area of the ceramic layer was increased through sol-treatment and the resulting specific surface area was between 20 and 25 m^2/g. The pore volume of the ceramic layer was in the region of 0.2 cm^3/g after the sol treatment. The ceramic layer was activated through impregnation with an aqueous solution of Pd (0.75 mol/l) and Pt (0.25 mol/l). The surface

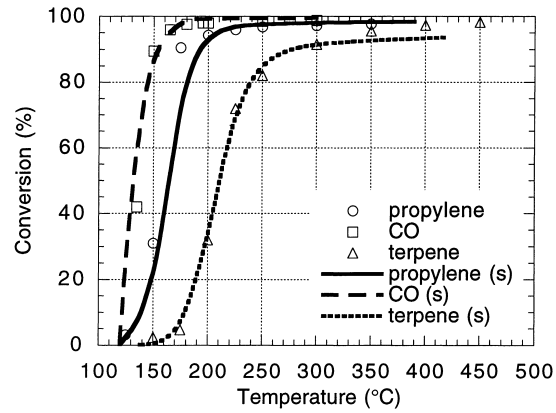

Fig. 4. Combustion of 2000 ppm of CO, propylene and terpenes over five catalytically active wire meshes in series (12 mesh×0.7 mm), gas flow: 420 m^3/m^2 h (STP), symbols represent experimental data whereas the lines represent simulated (s) data.

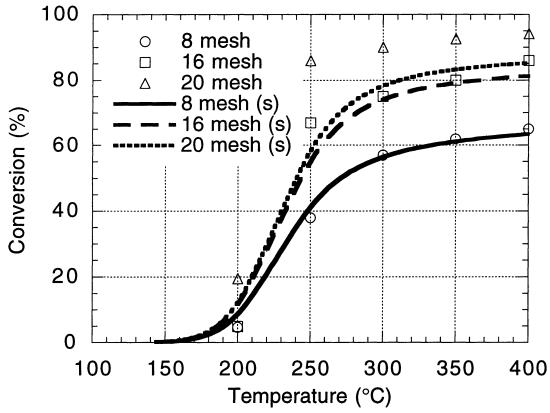

Fig. 5. Combustion of 2000 ppm of propylene over two catalytically active wire meshes in series (8, 16 and 20 mesh), gas flow: 420 m^3/m^2 h (STP), symbols represent experimental data whereas the lines represent simulated (s) data.

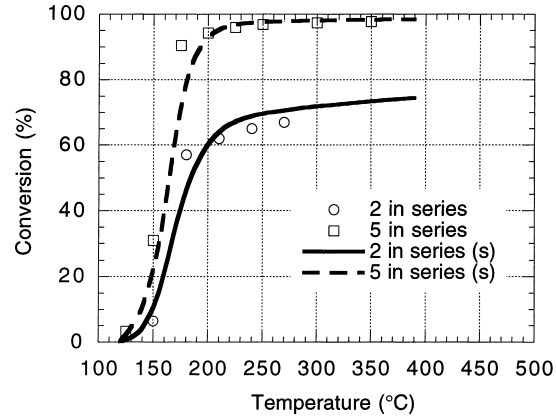

Fig. 6. Combustion of 2000 ppm of propylene over two and five catalytically active wire meshes in series (12 mesh×0.7 mm), gas flow: 420 m^3/m^2 h (STP), symbols represent experimental data whereas the lines represent simulated (s) data.

coverage of precious metals corresponded to the mono-layer capacity ($\sim$10 μmol/m^2).

The catalyst data and the experimental conditions were implemented in the model described earlier in this article and the conversion was calculated. In Fig. 4, the experimentally obtained conversions are compared to calculated data. As can be seen in the figure, the agreement between the calculated and the experimentally obtained data is excellent in the mass transfer controlled region.

The model thus describes the influence of the molecular weight and the gas-phase diffusivity in a correct way.

3.3.2. Influence of the mesh number

Catalytically active wire meshes with a mesh number ranging from 8 to 20 were studied. The wire meshes were coated with ceramic and active material in the same manner as in Section 3.3.1. In Fig. 5 the experimentally obtained conversion data for propylene combustion are compared to calculated data. The agreement is excellent in the cases of mesh numbers 8 and 16, whereas a difference between theory and practice is noticeable for mesh number 20. The model underestimates the conversion in this case. The difference may be attributed to increasing difficulties in obtaining a ceramic layer with an equal thickness as the mesh number increases. Increased thickness of the ceramic layer may increase the conversion and the pressure drop as the clear opening of the structure is decreased.

Despite the poor agreement for the tightest woven wire mesh the model enables a satisfactory prediction of the effects of the mesh number.

3.3.3. Influence of the number of wire meshes in series

In this case the number of catalytically active wire meshes (12 mesh) were varied during the combustion of propylene. As can be seen in Fig. 6, the agreement between experimental and calculated data is excellent. Thus, the model enables a good prediction of the effects of placing different numbers of catalytically active wire meshes in series.

3.3.4. Effects of the total flow

In this section we studied the effects of the flow on the propylene combustion when two catalytically active wire meshes (8 mesh) were placed in series. Again, it is evident that the model gives an excellent prediction of the conversion, see Fig. 7 where experimentally and calculated data are compared. In this study, the total flow was varied between 210 and 840 m^3/m^2 h (STP). In real applications the total flow may range from 1000 to above 10 000 m^3/m^2 h.

3.3.5. Experiments concerning the pressure drop

The pressure drop is modelled with the modified Ergun equation according to Eq. (16), where the bed porosity is

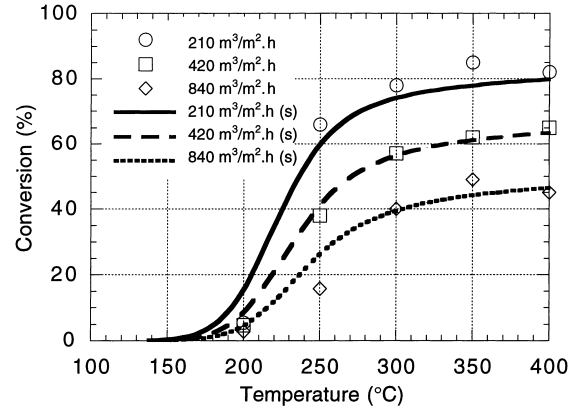

Fig. 7. Combustion of 2000 ppm of propylene over two catalytically active wire meshes in series (8 mesh×0.9 mm), gas flow: 210, 420 and 840 m^3/m^2 h (STP), symbols represent experimental data whereas the lines represent simulated (s) data.

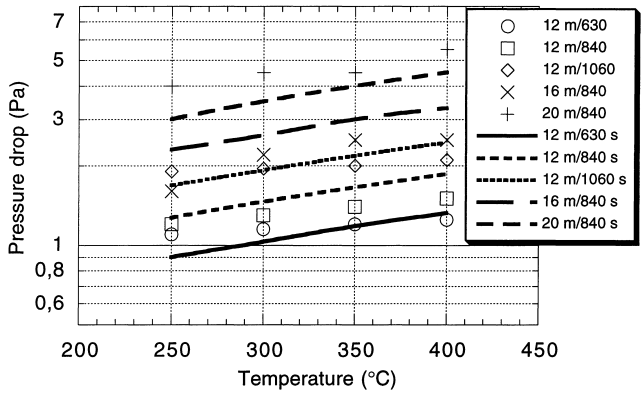

Fig. 8. The pressure drop versus the temperature for wire meshes with a mesh number ranging from 12 to 20, two wire meshes in series, gas flow: 630–1060 m^3/m^2 h (STP), symbols representing experimental data and lines representing simulated (s) data.

replaced with the structure porosity of the wire-mesh package. The experimentally obtained pressure drops and the corresponding calculated values are in fair agreement, as can be seen in Fig. 8.

3.4. Comparison of pellets-, monolith- and wire-mesh catalysts

3.4.1. Additional correlations for pellets- and monolith catalysts

The mass transfer coefficient in a packed bed can be determined through Eq. (20) according to Fogler [15]. Fogler also presents a correlation between the *j*-factor for mass transfer and the Reynolds number. A similar approach is presented by Carberry [16]. The mass transfer coefficient can easily be calculated from the *j*-factor and the dimensionless numbers. Although we are talking about correlations with a great inherent uncertainty, the mass transfer coefficient from these three analyses fall in a relatively narrow distribution (±10%).

$$Sh = 1.0\,Re^{1/2}\,Sc^{1/3}, \tag{20}$$

where

$$Sh = \frac{k_{ga} d_p}{D_g}\left(\frac{\epsilon_b}{1-\epsilon_b}\right)\frac{1}{\phi},\ Re = \frac{U d_p}{\nu(1-\epsilon_b)\phi},\ Sc = \frac{\nu}{D_g}.$$

The external surface area (a_{ext}) for a packed-bed catalyst is calculated from the following equation:

$$a_{ext} = \frac{6(1-\epsilon_b)}{\rho_p d_p}. \tag{21}$$

The situation is more complicated for monolith catalysts since the mass transfer coefficients calculated with different correlations presented may differ considerably. Cybulski et al. present a number of mass transfer correlations for monolith catalysts [19]. The channels of the monolith are assumed to have a square geometry.

$$Sh = 0.705\left(Re\frac{d_h}{L}\right)^{0.43} Sc^{0.56}, \tag{22a}$$

$$Sh = 0.766\left(Re\,Sc\frac{d_h}{L}\right)^{0.483}, \tag{22b}$$

$$Sh = 2.98\left(1 + 0.095 Re\,Sc\frac{d_h}{L}\right)^{0.45}. \tag{22c}$$

The Sherwood number will approach zero as the Reynolds number decreases according to Eqs. (22a) and (22b) whereas a limiting Sherwood number of 2.98 exists in Eq. (22c). Even if Eqs. (22a) and (22b) often are cited in the literature, Eq. (22c) is most likely to give correct results under reacting conditions, as indicated by Hayes and Kolaczkowski [20]. We therefore use Eq. (22c) in the calculation of *Sh*-numbers for monolith reactors.

The porosity of the monolith is calculated from the hydraulic diameter (d_h) and the wall-thickness (δ_w) according to the following equation:

$$\epsilon_m = \frac{d_h^2}{(d_h + \delta_w)^2}. \tag{23}$$

The external surface area ($a_{ext)}$ can be calculated from the porosity (ϵ_m) and the wall-thickness, δ_w, as described by Cybulski et al. [19].

$$a_{ext} = \frac{4(\sqrt{\epsilon_m} - \epsilon_m)A_c L}{\delta_w W}. \tag{24}$$

The Ergun equation is used to estimate the pressure drop for flow through a packed bed. According to this correlation the pressure drop is dependent upon the superficial velocity, the length of the packed bed, the porosity of the packed bed, the sphericity of the particles in the bed (ϕ) and the density of the fluid (ρ) [21].

$$\Delta p = \rho U^2 \frac{L}{\phi d_p}\frac{1-\epsilon_b}{\epsilon_b^3}\left(\frac{150}{Re_p} + 1.75\right), \tag{25}$$

where

$$Re_p = \frac{\phi d_p U}{\nu(1-\epsilon_b)}.$$

For the monolith catalyst, the pressure drop may be calculated by Darcy–Weisbach equation [19]. In this case laminar flow conditions are assumed and the pressure drop is calculated from the superficial gas velocity, the length of the monolith, the hydraulic diameter and the density of the fluid. The friction coefficient is taken as 64/*Re*, which is valid for a perfectly laminar flow.

$$\Delta p = \lambda\frac{L}{d_h}\frac{\rho U^2}{2}, \tag{26}$$

where λ=64/*Re* and Re=$d_h U/\nu$.

3.4.2. Correlations for calculating the thermal response

The thermal response (*T*) is defined as the ratio between the thermal inertia (ΓV_{cat}) and the total heat transfer capa-

city (αa_{ext}):

$$T = \frac{\Gamma V_{cat}}{\alpha a_{ext}}. \quad (27)$$

The specific thermal inertia for a packed-bed catalyst corresponds to:

$$\Gamma = \rho_b c_{ps}. \quad (28)$$

In the monolith catalyst, the porosity of the structure must be taken into consideration:

$$\Gamma = (1 - \epsilon_m)\rho_w c_{ps}. \quad (29)$$

The wire-mesh catalyst consists of a wire-mesh structure and a ceramic layer. The resulting density (ρ_r) is calculated from Eq. (31). The specific thermal inertia can then be calculated from the wire-mesh porosity, the resulting density and the thermal capacity (c_{ps}):

$$\Gamma = (1 - \epsilon_w)\rho_r c_{ps}, \quad (30)$$

$$\rho_r = \frac{d^2\rho_{wi} + (d_t^2 - d^2)\rho_c}{d_t^2}. \quad (31)$$

3.4.3. Evaluation parameters

It is now interesting to compare the characteristics of different catalysts. There are a couple of features which are important in most catalytic applications:

- catalyst performance relative to the catalyst volume
- catalyst performance relative to the pressure drop
- catalyst performance relative to the geometric weight of the catalyst
- catalyst performance relative to the catalyst weight
- thermal response

The evaluation parameters are made independent of the conversion by placing $\ln(1-x_A)$ in the numerator, which is valid for a first-order reaction in the absence of axial dispersion. Parameter A represents the catalyst performance relative to the catalyst volume, B the catalyst performance relative to the catalyst weight, C the catalyst performance relative to the geometric weight (i.e. the total weight of the catalyst, geometric substrate included), D the catalyst performance relative to the pressure drop. Parameter E represents the inverted thermal response. The numbers of the parameters should in all cases be as high as possible.

$$A = -\frac{\ln(1 - x_A)}{V_{cat}} \ (m^{-3}), \quad (32)$$

$$B = -\frac{\ln(1 - x_A)}{W} \ (kg^{-1}), \quad (33)$$

$$C = -\frac{\ln(1 - x_A)}{m_{cat}} \ (kg^{-1}), \quad (34)$$

$$D = \frac{\ln(1 - x_A)}{\Delta P} \ (Pa^{-1}), \quad (35)$$

$$E = \frac{1}{T} = \frac{\alpha a_{ext}}{\Gamma V_{cat}} \ (s^{-1}). \quad (36)$$

Table 1
Catalyst dimensions used in the comparison study

Monolith catalyst		Wire-mesh catalyst		Pellets d_p (mm)
cpsi (in^{-2})	δ_w (mm)	N (mesh no.)	d (mm)	
400	0.2	32	0.3	0.25
100	0.4	20	0.5	1.0
50	0.6	12	0.7	4.0
12	1.1	4	1.65	

The catalyst volume necessary for a certain degree of conversion is thus inversely proportional to the evaluation parameter A. If the evaluation parameter A is increased by a factor 2, the catalyst volume necessary for that particular degree of conversion will be decreased by a factor 2. The other evaluation parameters are correlated in the same manner.

3.4.4. Assumptions

It is interesting to compare the performance of different catalysts by use of the evaluation parameters described above.

The cross-section area of the reactor was assumed to be 0.1 m^2 and calculations were performed for CO-combustion at the following flow rates: 5000 and 20 000 m^3/m^2 h (STP). The catalyst alternatives studied are given in Table 1. Isothermal conditions were assumed.

The monoliths were assumed to be coated with a wash-coat of a thickness of 25 μm. The wash coat was assumed to have a specific surface area of 100 m^2/g and a total pore volume of 0.75cm^3/g. The content of precious metals corresponded to 10% of the mono-layer capacity. The wall density (ρ_w) was taken as 2000 kg/m^3 and the length of the monoliths were 0.2 m.

The thermally sprayed ceramic layer (25 μm) was assumed to have a specific surface area of 25 m^2/g and a total pore volume of 0.2 cm^3/g. The content of precious metals corresponded to 50% of the monolayer capacity to compensate for the relatively low specific surface area.

The pellets catalyst was assumed to consist of porous spherical particles of alumina with a specific surface area of 100 m^2/g and a total pore volume of 0.75 cm^3/g. The content of precious metals corresponded to 10% of the mono-layer capacity, as in the wash coat of the monolith. The precious metals are assumed to be evenly distributed throughout the pellets. The particle density (ρ_p) was taken as 940 kg/m^3.

3.4.5. Performance relative to the catalyst volume

In Fig. 9, the evaluation parameter A (catalyst performance relative to the catalyst volume) is presented for the different catalysts at different flow rates. The pellets catalyst with the smallest particle diameter is superior to the other catalysts. The performance of the pellets catalyst is however sensitive to the particle diameter, mainly attributed to the effects of pore diffusion. The monolith catalyst is inferior to both pellets- and wire-mesh catalysts. From the figure it is

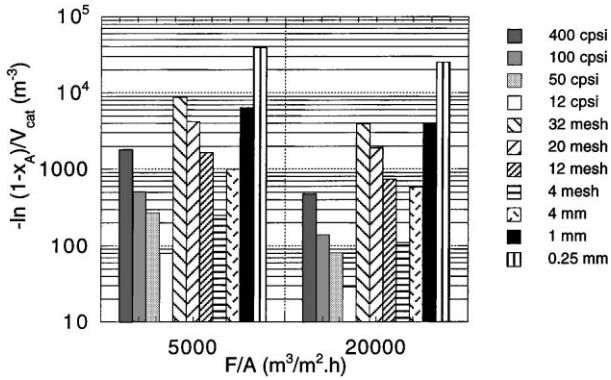

Fig. 9. Presentation of the evaluation parameter – $\ln(1-x_A)/V_{cat}$ for different catalyst alternatives, gas flow: 5000 and 20 000 m^3/m^2 h (STP). Monolith catalyst: 12, 50, 100 and 400 cells per square inch (cpsi); wire-mesh catalyst: 4, 12, 20 and 32 meshes per inch (mesh); pellet catalyst: 0.25, 1.0 and 4.0 mm in diameter (mm).

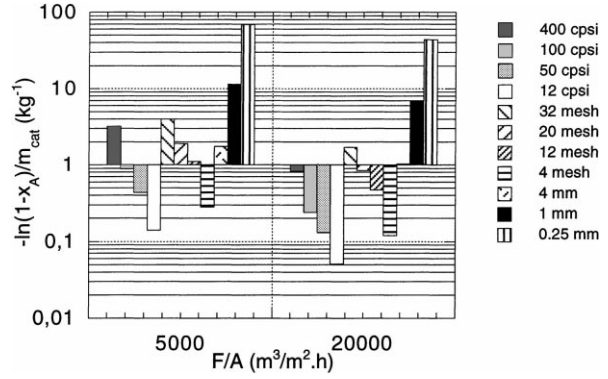

Fig. 11. Presentation of the evaluation parameter – $\ln(1-x_A)/m_{cat}$ for different catalyst alternatives, gas flow: 5000 and 20 000 m^3/m^2 h (STP). Monolith catalyst: 12, 50, 100 and 400 cells per square inch (cpsi); wire-mesh catalyst: 4, 12, 20 and 32 meshes per inch (mesh); pellet catalyst: 0.25, 1.0 and 4.0 mm in diameter (mm).

evident that it is possible to reduce the reactor volume by a factor 10 or more by replacing monolith catalysts with an appropriate pellets- or wire-mesh catalyst, based on this criterion only.

3.4.6. Performance relative to the catalyst weight and the total weight

The catalyst utilisation is an important factor to take into consideration. Evaluation parameter *B* describes the catalyst performance relative to the catalyst weight (only active catalyst). The catalyst utilisation is poor in the case of a pellets catalysts with a large particle diameter, as can be seen in Fig. 10. The catalyst utilisation is however greatly improved when the particle diameter is reduced, mainly attributed to decreased effects of pore diffusion. The catalyst utilisation is generally somewhat higher for a wire-mesh catalyst compared to a monolith catalyst. This fact is attributed to the poor mass transfer characteristics of a monolith catalyst which must be compensated for by an increased contact area between the fluid and the catalyst.

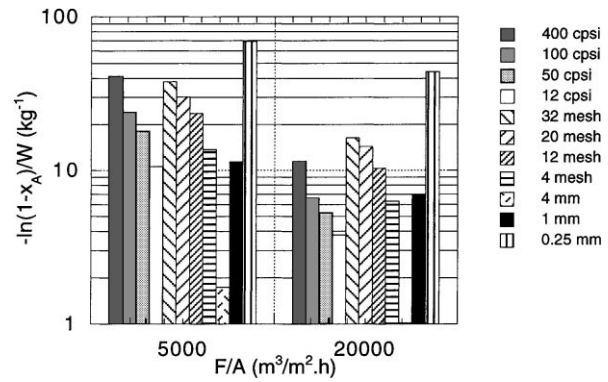

Fig. 10. Presentation of the evaluation parameter – $\ln(1-x_A)/W$ for different catalyst alternatives, gas flow: 5000 and 20 000 m^3/m^2 h (STP). Monolith catalytst: 12, 50, 100 and 400 cells per square inch (cpsi); wire-mesh catalyst: 4, 12, 20 and 32 meshes per inch (mesh); pellet catalytst: 0.25, 1.0 and 4.0 mm in diameter (mm).

This will also lead to an increased amount of catalyst (at a constant thickness of the catalyst layer).

In the case of a pellets catalyst no geometrical substrate exists (i.e. wall or wire-mesh structure). A geometrical substrate will contribute to the total mass of the catalyst and will decrease the catalyst performance relative to the geometric weight, as indicated by evaluation parameter *C*. In Fig. 11 the catalyst performance relative to the geometric weight is presented at different flows. The pellets catalyst has generally higher value of this evaluation parameter than the other two alternatives. The monolith catalyst has throughout the lowest values.

3.4.7. Performance relative to the pressure drop

In addition to the volume effectiveness the pressure-drop characteristics will be one of the most important factors to take into consideration in most applications (e.g. in automotive applications). Evaluation parameter *D* presents the catalyst performance relative to the pressure drop. From Fig. 12 it is evident that monolith catalysts are superior in this sense whereas pellets catalysts give the highest pressure drops. Wire-mesh catalysts have a pressure-drop performance in between monolith- and pellets catalysts.

3.4.8. Thermal response

The thermal response of the catalyst is important in many applications, e.g. in automotive applications. The thermal response is improved when the external surface area and the heat transfer numbers are increased or when the thermal inertia is decreased. These characteristics are summarised in evaluation parameter *E*, which describes the initial temperature gain of the catalyst when subjecting it to hot gases. As can be seen in Fig. 13 the pellets catalyst is superior to the monolith- and the wire-mesh catalysts. This is attributed to the large external surface area of the pellets catalyst in combination with high heat transfer number and a relatively low thermal inertia. The thermal response of the wire-mesh

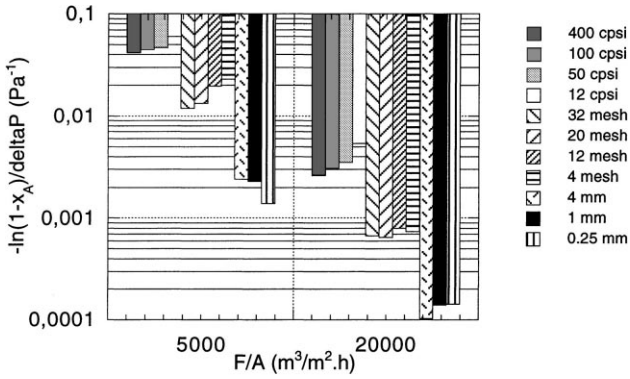

Fig. 12. Presentation of the evaluation parameter – $\ln(1-x_A)/\Delta p$ for different catalyst alternatives, gas flow: 5000 and 20 000 m^3/m^2 h (STP). Monolith catalyst: 12, 50, 100 and 400 cells per square inch (cpsi); wire-mesh catalyst: 4, 12, 20 and 32 meshes per inch (mesh); pellet catalyst: 0.25, 1.0 and 4.0 mm in diameter (mm).

catalyst is however generally 2–3 times higher than the corresponding values of the monolith catalysts.

4. Conclusions

The mass transfer correlations proposed by other researchers are valid also for catalytically active wire-meshes, prepared through thermal spraying, as shown in this study. The numerical model described in the paper makes it possible to predict conversion data and pressure drops with a high degree of accuracy.

The mass- and heat transfer characteristics of a wire-mesh catalyst is comparable to the mass- and heat transfer characteristics of a packed bed. Correspondingly the catalyst volume can be reduced greatly compared to a monolith catalyst where laminar flow conditions normally prevail in the channels. The mass- and heat transfer numbers will increase as the mesh number is increased.

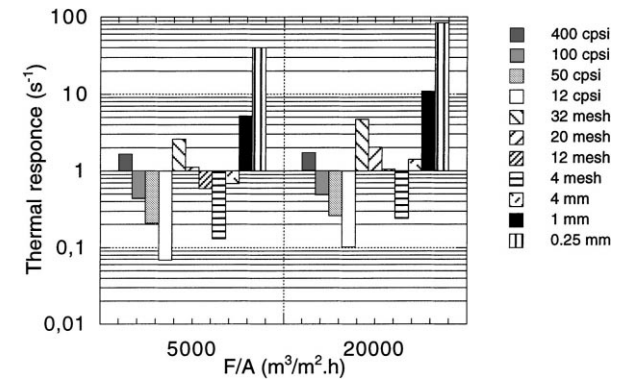

Fig. 13. Presentation of the evaluation parameter $\alpha\, a_{ext}/\Gamma V_{cat}$ for different catalyst alternatives, gas flow: 5000 and 20 000 m^3/m^2 h (STP). Monolith catalyst: 12, 50, 100 and 400 cells per square inch (cpsi); wire-mesh catalyst: 4, 12, 20 and 32 meshes per inch (mesh); pellet catalyst: 0.25, 1.0 and 4.0 mm in diameter (mm).

The ceramic layer of a thermally sprayed wire-mesh catalyst has a shell-like appearance which means that the effects of pore diffusion will be small.

The effects of axial dispersion are normally insignificant except when using large wire or pellets diameters at high conversions (>95%). The reactor may thus be modelled as a plug-flow reactor without introducing significant errors.

The pressure drop of a package of wire-meshes is somewhat higher than the pressure drop of a monolith. The increased pressure drop is however insignificant in most practical applications. The relatively low pressure drop of wire-mesh catalyst is attributed to the high porosity of the structure (often above 70%).

The thermal losses due to radial conduction will be vanishingly low due to the low circumference area of a package of catalytically active wire meshes. The radial temperature gradient over the wire mesh is thus expected to be negligible. The absence of severe radial temperature gradients in wire-mesh catalysts will lead to a quicker start-up of the catalyst, which is of importance in many applications.

The wire-mesh catalyst has a better thermal response than a monolith catalyst, attributed to higher heat transfer numbers and a lower thermal inertia. Calculations and experimental studies show that the initial temperature gain when subjecting a wire-mesh catalyst for hot gases is 2–3 times higher than the corresponding temperature gain of a monolith catalyst. This fact in combination with the negligible radial temperature gradients will give a superior ignition characteristic of the wire-mesh catalyst.

The geometric flexibility offered by the wire-mesh catalysts is one of the most important features. It is possible to design a wire-mesh catalyst for almost any catalytic application and to fit into almost any geometry. The preparation method for the catalyst will be similar in all cases. One important area of application will be retro-fit installation of systems for flue-gas cleaning where geometrical aspects up to now have prevented installation.

The thermally sprayed catalyst has an excellent thermal and mechanical strength. Thermally sprayed layers are normally used as thermal barriers in rocket engines where the temperature and pressure conditions are extremely severe. The thermally and mechanically induced strains will be much lower in catalyst applications. The resistance towards thermal deactivation is dependent upon the stabilisation of the surface increasing material and the choice of active material.

The implementation of wire-mesh catalysts has up to now been prevented due to poor catalyst performance (wash coated wire meshes) and high catalyst cost (homogeneous wire meshes of precious metals). The preparation method indicated in this paper opens a new way of producing a relatively cheap catalyst for a wide variety of applications:

- Flue gas cleaning (stationary sources)
- Automotive applications (two- and three-way catalysis)

- Energy production (catalytic combustion)
- Ammonia oxidation
- Selective reduction of nitrogen oxides (SCR)
- Steam reforming and water-gas reactions
- Partial oxidation for chemical production

Wire-mesh catalysts might, however, be sensitive to poisoning since they only contain a small amount of catalytically active phase. Due to the high mass transfer numbers in such structures the poisons will also be transported to the catalyst layer very effectively. Clogging effects might be another severe problem if the gas contains high concentrations of particulate matter.

The continued research work will therefore be focused on catalyst deactivation. The objective is to get a fundamental understanding of how catalytically active wire meshes are deactivated in different applications.

5. Nomenclature

Dimensionless numbers

J_D	*j*-factor for mass transfer
J_h	*j*-factor for heat transfer
Pr	Prandtl number
Re	Reynolds number
Sc	Schmidt number
Sh	Sherwood number

Variable

A	ratio between catalyst performance and catalyst volume
A_c	cross-section area of catalyst (m^2)
a_{ext}	external surface area of catalyst (m^2/kg)
B	ratio between catalyst performance and catalyst weight
C	ratio between catalyst performance and total weight of catalyst
C_A	concentration of component *A* (mol/m^3)
C_{Ao}	inlet concentration of component *A* (mol/m^3)
c_{pa}	heat capacity of air (J/kg K)
c_{ps}	heat capacity of solid (J/kg K)
D	ratio between catalyst performance and pressure drop
d	wire diameter (m)
D_a	axial dispersion coefficient (m^2/s)
D_{eff}	effective diffusion coefficient (m^2/s)
D_g	diffusion coefficient in the gas phase (m^2/s)
d_h	hydraulic diameter of channels in the monolith (m)
D_k	Knudsen diffusion coefficient (m^2/s)
d_p	particle diameter (m)
d_t	diameter of wire coated with ceramic material (m)
E	ratio between heat transfer capacity and thermal inertia
E_a	activation energy (J/mol)
k	rate coefficient (1/s)
k_0	pre-exponential factor (mol/s kg Pa)
k_{ga}	mass transfer coefficient (m/s)
k_v	$r_{int}/C_A\ S_a$=rate coefficient (m^3/m^2 s)
l	length coordinate (m)
m_{cat}	geometric weight (kg)
MW	molecular weight
N	mesh number (m^{-1})
Nc	cell density of the monolith (m^{-2})
n	number of wire meshes in series
L	length of catalyst (m)
p_{HC}	partial pressure of hydrocarbons (Pa)
p_{O_2}	partial pressure of oxygen (Pa)
r_{int}	intrinsic reaction rate (mol/s kg)
r_{obs}	observed reaction rate (mol/s kg)
S_a	specific surface area (m^2/kg)
T	temperature (K)
t	volume of catalyst/exterior surface available for reactant penetration and diffusion
$\bar{t}$	residence time (s)
t_c	thickness of catalyst layer (m)
U	superficial gas velocity (m/s)
V_0	volume flow (m^3/s)
V_{cat}	catalyst volume (m^3)
V_p	total pore volume (m^3/kg)
W	catalyst weight (kg)
x_A	conversion
z	dimensionless length

Greek letters

α	heat transfer number (W/m^2 K)
ΔH	reaction enthalpy (J/mol)
Δp	pressure drop (Pa)
δ_w	wall thickness (m)
ϵ_m	porosity of the monolith
ϵ_b	bed porosity
ϵ_w	porosity of wire mesh
Φ	Thiele modulus
ϕ	sphericity
Γ	specific thermal inertia (J/m^3 K)
λ	friction factor
λ_a	thermal conductivity of air (W/m K)
λ_p	thermal conductivity of solid (W/m K)
ν	kinematic viscosity (m^2/s)
ϵ_p	particle porosity
θ_{PM}	coverage of active material (mol/m^2)
ρ	air density (kg/m^3)
ρ_b	bulk density (kg/m^3)
ρ_c	density of catalyst layer (kg/m^3)
ρ_p	particle density (kg/m^3)
ρ_r	resulting density (kg/m^3)
ρ_w	wall density (kg/m^3)

ρ_{wi} density of wire (kg/m^3)
T characteristic temperature response (s)
τ tortuosity factor, normally 3–4
Ω overall effectiveness factor

References

[1] N. Arashi, Y. Hishinuma, K. Narato, F. Nakajima, H. Kuroda, Int. Chem. Eng. 22(3) (1982) 489–494.
[2] R. Prasad, L.A. Kennedy, E. Ruckenstein, Catal. Rev. -Sci. Eng. 26(1) (1984) 1–58.
[3] M.F.M. Zwinkels, S.G. Järås, P.G. menon, T.A. Griffin, Catal. Rev.-Sci Eng. 35(3) (1993) 319.
[4] C.N. Satterfield, Heterogeneous Catalysis in Practice, McGraw-Hill, New York, 1980, p. 219.
[5] A.B. Stiles, T.A. Koch, Catalyst Manufacture, Marcel Dekker, New York, 1999, p. 200.
[6] W.F. Maier, J.W.A. Schlangen, Catal. Today 17 (1993) 225–234.
[7] A. Kapoor, S.K. Goyal, N.N. Bakhsni, Can. J. Chem. Eng. 64(5) (1986) 792–802.
[8] W.J. Thomsom, J.M. Arndt, K.L. Wright, Am. Chem. Soc., Div. Fuel Chem. 25(2) (1979) 101–118.
[9] H.W. Pennline, R.R. Schehl, W.P. Haynes, Ind. Eng. Chem. Proc. Des, Dev. 18(1) (1979) 156–162.
[10] M.J. Baird, F.W. Steffgen, Ind. Eng. Chem. Prod. Res. Dev. 16(2) (1977) 142–147.
[11] W.P. Haynes, J.J. Elliott, A.J. Forney, Am. Chem. Soc. Div. Fuel. Chem. 16(2) (1972) 47–63.
[12] B.I. Loran, J.B. O'Hara, Environ. Sci. Technol. 12(12) (1978) 1258–1263.
[13] T. Yoneshige, R. Nakajima, JP 61291718 A2 861222 to Nissan Motor.
[14] C.N. Satterfield, D.H. Cortex, Ind. Eng. Chem. Fundam. 9(4) (1970) 613–620.
[15] H.S. Fogler, Elements of Chemical Reaction Engineering, Prentice-Hall, NJ, 1986.
[16] J.J. Carberry, Chemical and Catalytic Reaction Engineering, McGRaw-Hill, New York, 1976.
[17] A.F. Ahlström-Silversand, C.U.I. Odenbrand, Appl. Catal. A 153 (1997) 177–201.
[18] O. Levenspiel, Chemical Reaction Engineering, Wiley, New York, 1972.
[19] A. Cybulski, J.A. Moulijn, Catal. Rev.-Sci. Eng. 36(2) (1994) 179–270.
[20] R.E. Hayes, S.T. Kolaczkowski, Chem. Eng. Sci. 49(21) (1994) 3587–3599.
[21] J.M. Coulson, J.F. Richardson, Chemical Engineering, vol. 2 – Unit Operations, Pergamon Press, New York, 1978, p. 131.
[22] L.P.B.M. Janssen, M.M.C.G. Warmoeskerken, Transport Phenomena Data Companion, Edward Arnold, London, 1987, p.78.